J. Math. Biol. 43, 221–246 (2001)
Digital Object Identifier (DOI):
10.1007/s002850000078

Mathematical Biology

F. Berezovskaya · G. Karev · R. Arditi

Parametric analysis of the ratio-dependent predator–prey model

Received: 24 December 1999 / Revised version: 27 October 2000 /
Published online: 21 August 2001 –

Abstract. We present a complete parametric analysis of stability properties and dynamic regimes of an ODE model in which the functional response is a function of the ratio of prey and predator abundances. We show the existence of eight qualitatively different types of system behaviors realized for various parameter values. In particular, there exist areas of coexistence (which may be steady or oscillating), areas in which both populations become extinct, and areas of "conditional coexistence" depending on the initial values. One of the main mathematical features of ratio-dependent models, distinguishing this class from other predator–prey models, is that the Origin is a complicated equilibrium point, whose characteristics crucially determine the main properties of the model. This is the first demonstration of this phenomenon in an ecological model. The model is investigated with methods of the qualitative theory of ODEs and the theory of bifurcations. The biological relevance of the mathematical results is discussed both regarding conservation issues (for which coexistence is desired) and biological control (for which extinction is desired).

1. Introduction

The construction and study of models for the population dynamics of predator–prey systems have remained an important area in theoretical ecology since the famous Lotka-Volterra equations. These authors set a framework which is still followed today: a system of two differential equations, with a simple correspondence (usually proportionality) between prey consumption and predator production. A most crucial element in these models is the "functional response" or "trophic function", the function that describes the number of prey consumed per predator per unit time for given quantities of prey N and predators P.

Much early work was only concerned with the way in which this function varies with prey density (e.g., the so-called Holling types I, II, III), ignoring the effect of predator density. Even today, most simulation models developed for applications

F. Berezovskaya, G. Karev: Center for Problems of Forest Ecology and Productivity, Russian Academy of Sciences, 62 Novocheremushkinskaya str., Moscow 117418, Russia. e-mail: fsberezo@hotmail.com; gkarev@hotmail.com. Current address: School of Mathematics, Georgia Institute of Technology, Atlanta, GA 30332, USA

R. Arditi (author for correspondence): Institut National Agronomique Paris-Grignon, Ecologie des Populations et Communautés, 16 rue Claude Bernard, 75231 Paris Cedex 05, France. e-mail: arditi@inapg.inra.fr

Key words or phrases: Dynamical system – Phase portrait – Bifurcation – Complicated singular point – Population dynamics – Biological control

assume that the trophic function is a function of prey density only. This was labeled "prey-dependence" by Arditi and Ginzburg (1989).

It is known that only stable equilibrium coexistence of predators and prey or extinction of predators are possible in the framework of the "classical" Lotka-Volterra model with quadratic (logistic) prey growth. An additional regime of oscillating coexistence can arise in various models with saturation of the trophic function (e.g., Rosenzweig 1971, Bazykin 1998).

Note that such models cannot describe the experimental observations (e.g., Huffaker 1958, Luckinbill 1973) that, with given values of system parameters, the predator population or both populations can either become extinct or coexist, depending on the initial population values. Moreover, the extinction can be accompanied by oscillations. Additionally, simple prey-dependent models cannot produce situations of biological control, i.e., durable coexistence of a pest (the prey) with its predator at a mean abundance being much lower than the prey carrying capacity (Luck 1990). This was labelled "paradox of biological control" (Arditi and Berryman 1991).

It was recognized early that the predator density could have a direct effect on the trophic function. A number of such "predator-dependent" models (in the sense of Arditi and Ginzburg 1989) have been proposed, the most widely known being those of Hassell and Varley (1969), DeAngelis et al. (1975), or Beddington (1975).

Arditi and Ginzburg (1989) have suggested that the essential properties of predator-dependence could be rendered by a simpler form which was called "ratio-dependence". The trophic function is assumed to depend on the single variable N/P rather than on the two separate variables N and P. When considered in community-level situations (i.e., food chains and food webs), it was shown that ratio-dependent models make more reasonable predictions than their prey-dependent counterparts (Arditi and Berryman 1991, Arditi et al. 1991, Hanski 1991, Michalski and Arditi 1995, Arditi and Michalski 1996).

The ratio-dependent hypothesis has aroused a heated controversy (e.g., Ruxton and Gurney 1992, Arditi et al. 1992, Abrams 1994, Diehl et al. 1994, Sarnelle 1994, Akçakaya et al. 1995), mainly due to the fact that, at first, the main arguments were phenomenological. However, a number of mechanistic models have now shown how ratio-dependent (or, more generally, predator-dependent) trophic functions can emerge on the global scale with the local law of interaction still being the prey-dependent Lotka-Volterra model. Spatial and/or temporal heterogeneities are essential ingredients of these mechanistic models (Michalski et al. 1997, Poggiale et al. 1998, Cosner et al. 1999). Fortunately, the controversy seems to be coming to a more moderate level, with both parties agreeing on a number of basic points and recognizing some merits in both approaches (Abrams and Ginzburg 2000).

From the mathematical point of view, ratio-dependent predator–prey models raise delicate questions because the functional response is undefined at the origin $N = 0$, $P = 0$. As a consequence, the origin is a so-called "complicated point", as it will be shown here. Ratio-dependent models can display original dynamic properties that have never been observed in earlier simple two-dimensional predator–prey models. For example, the origin can be a node simultaneously attractive and repulsive, thus shedding new light on ecological extinction, particularly in the context

of biological control. Coexistence of several dynamic regimes with the same set of parameters can also be observed. These are realistic features since, as mentioned above, these behaviors have been observed experimentally.

Several authors have examined specific mathematical properties of the model, However, these studies either contained errors (Freedman and Mathsen 1993) or were only partial (Kuang and Beretta 1998, Beretta and Kuang 1998, Kuang 1999, Jost et al. 1999). A complete parametric analysis of stability properties and dynamic regimes had not been achieved until now. This will be the purpose of the present paper.

2. The ratio-dependent model and its parameterization

The general ratio-dependent prey-predator model of Arditi and Ginzburg (1989) is

$$\begin{aligned} N_t &= rN\varphi(N) - g(N/P)P \\ P_t &= eg(N/P)P - qP \end{aligned}$$

where the function $rN\varphi(N)$ characterizes the velocity of prey growth in the absence of predators, the linear function qP describes the velocity of predator death in the absence of prey and the function $g(x) = g(N/P)$ is the trophic function. The more specific form of this model in the present paper assumes the familiar logistic form for $N\varphi(N)$ and the Monod-Holling hyperbolic form for $g(x) = \alpha x/(1 + \alpha hx) = \alpha N/(P + \alpha hN)$, where $(N, P) \in [0, \infty)^2 \backslash (0, 0)$, $G(N > 0, 0) = 1/h$, $G(0, P > 0) = 0$ (Jost et al. 1999).

So, we shall study the system

$$\begin{aligned} N_t &= rN(1 - N/K) - \alpha NP/(P + \alpha hN) \\ P_t &= e\alpha NP/(P + \alpha hN) - qP \end{aligned} \tag{1}$$

Besides the densities of prey and predator populations N and P, the parameters of the system are the non-negative values r, K, α, h, e, q. Here r and K characterize, respectively, the growth rate and the carrying capacity of the prey population in the absence of the predator, q is the predator natural mortality rate; e is the conversion efficiency of predators. The parameters α and h characterize the ratio-dependent trophic function: h is the predator handling time and α is the maximum prey consumption rate.

With appropriate changes of variables $(N, P, t) \to (x, y, \tau)$, the model can be simplified to a dimensionless form with a reduced number of independent parameters. This makes the mathematical analysis easier while preserving the essential problems. There exist several formally equivalent different dimensionless forms having three parameters (which is, in the present model, the lowest possible number). The choice of the form and the specific combination of r, K, α, h, e, q as new parameters are essentially defined by the ecological goal of the study.

In the present paper, our goal is to study the ratio-dependent system mainly in its dependence on the predator population, i.e., for changes of parameters that characterize the trophic relations. This leads to the following reduction of model (1):

$$N = Kx, \quad P = K\alpha hy, \quad t = \tau/r \tag{2}$$

with the parameters:

$$\nu = \alpha/r,\ \mu = e/(rh),\ \gamma = q/r \tag{3}$$

and the dynamic equations

$$\begin{aligned} x_\tau &= x(1-x) - \nu xy/(x+y) \\ y_\tau &= -\gamma y + \mu xy/(x+y) \end{aligned} \tag{4}$$

The parameter γ represents the death rate of the re-defined predators y. The "trophic components" are characterized by the two parameters ν and μ which have the following meaning. ν is the maximum (asymptotic) prey death rate due to predation, for an infinite number of predators; for short, it will be called "the consumption ability". μ is the maximum (asymptotic) predator growth rate for an infinite number of prey; for short, it will be called "the predator growing ability".

Note that in the work of Jost et al. (1999), model (1) was reduced to a different form from (2–4) that was appropriate in order to analyze the system mainly in its dependence on prey characteristics under fixed trophic characters. It is significant that both reductions are equivalent mathematically (see Appendix 4) but serve different and complementary ecological goals.

In the rest of this paper, we shall study the dynamics of model (4) in its dependence on parameters (μ, ν, γ). Section 3 contains the formulation of the main mathematical results of the investigation of system (4), formalized in Theorem A. Sections 4–6 as well as Appendices A1–A4 are devoted to the proof of this Theorem. Interpretations of the outcomes and a discussion are in Sections 7 and 8.

3. Purpose of the work and main result

The purpose of the mathematical study of system (4) is to describe completely its qualitative behavior in a finite part of the first quadrant of the plane (x, y), and its dependence on the positive parameters γ, μ, ν. For this, we divide the parameter space into domains corresponding to topologically different phase portraits of system (4) in such way that boundaries between the parameter domains correspond to the bifurcations of the system.

The system (4) has in the first quadrant the equilibrium points $\boldsymbol{O}(x = 0, y = 0)$ and $\boldsymbol{A}(x = 1, y = 0)$ for all parameter values. Additionally, for some parameter values, the system can have a nontrivial equilibrium point $\boldsymbol{B}(x = x^*, y = y^*)$ (see Section 4.1) and a limit cycle "born" from this point (see Section 4.3).

Moreover, one of the main mathematical peculiarities of ratio-dependent models, distinguishing this class from many other predator–prey models, is that the origin $\boldsymbol{O}$ is a *complicated equilibrium point for all parameter values*. As we show below, the main peculiarities of system (4) are essentially determined by the characteristics of point $\boldsymbol{O}$.

The main result is the following.

Theorem A. *The space of parameters* (γ, μ, ν) *is subdivided into* 8 *domains of topologically different phase portraits in the finite part of the positive quadrant of*

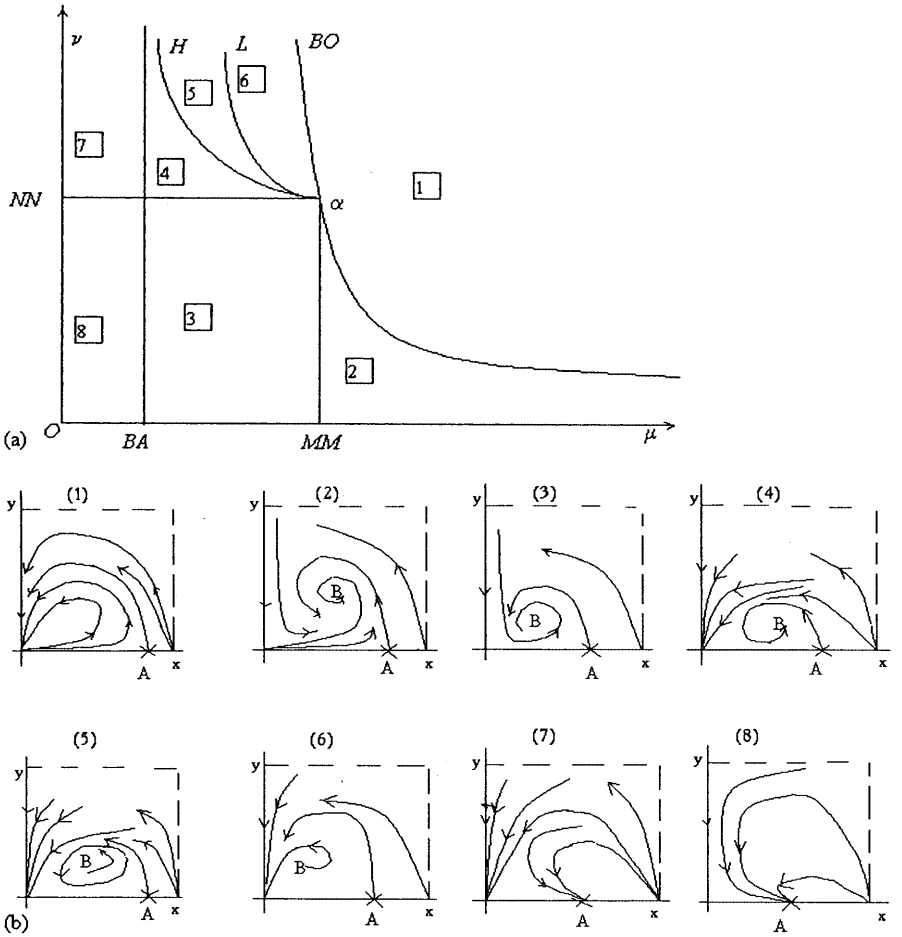

Fig. 1. Bifurcation diagram of model (4). (a) The parametric portrait of the model in the plane (μ, ν) for a "typical" value of parameter γ consists of 8 domains. The boundaries correspond to the following bifurcations. (i) ***BO*** and ***BA***: appearance/disappearance of the nontrivial equilibrium point ***B***; (ii) ***H***: Andronov-Hopf supercritical bifurcation of point ***B***; (iii) ***MM*** and ***NN***: changes in the topological structure of the trivial equilibrium point ***O***; (iv) ***L***: appearance/disappearance of a limit cycle at the heteroclinic bifurcation of the separatrices of points ***O*** and ***A***. (b) Phase portraits corresponding to the parametric domains.

the plane (x, y) (*Fig. 1a, b*). *The boundary surfaces between domains correspond to the following bifurcations in system* (4):
BO*:* $\nu = \mu/(\mu - \gamma)$, ***BA****:* $\mu = \gamma$ *– appearance/disappearance of the nontrivial equilibrium point* ***B*** (*see Fig. 2*);
MM*:* $\mu = \gamma + 1$, $\nu < \gamma + 1$, ***NN****:* $\nu = \gamma + 1$, $\mu < \gamma + 1$ *– changes of topological structure of the equilibrium point* ***O*** *in the first quadrant under which a node sector appears/disappears in a vicinity of the point* ***O***;
H*:* $\nu = \mu(\gamma+\mu/(\mu-\gamma))/(\mu+\gamma)$, $\gamma < \mu < \gamma+1$ *– Andronov-Hopf supercritical bifurcation of the point* ***B***;

Table 1. Example of parameter values that set the system in each of the eight domains of Fig. 1.

Domain	**1**	**2**	**3**	**4**	**5**	**6**	**7**	**8**
μ	3	3	2	2	2.1	2.2	1	1
ν	2	1	1	2.7	2.92	2.92	2.7	1

L *– heteroclinics formed by separatrices of the points* ***A*** *and* ***O***. (*This boundary corresponds to a non-local bifurcation and was obtained by computation*).

For parameter values α*:* $\nu = \gamma + 1 = \mu$*, the system* (4) *has a first integral of the form*:

$$(\gamma + 1)ln((x + y)/x) - y(1 + \gamma/x) = C, \tag{5}$$

where C is an arbitrary constant.

All boundary surfaces correspond to bifurcations of co-dimension[1] 1 in system (4). The lines of intersection or touching between the boundary surfaces correspond to bifurcations of co-dimension 2. Figure 1a represents the 3-dimensional parameter portrait of the system as a cross-section into the plane (μ, ν) for some arbitrarily fixed typical value of parameter γ. In this cross-section, surfaces between domains appear as boundary curves and common lines of these surfaces appear as points of intersection or touching of the curves.

The proof of the Theorem is provided by the analytical as well as numerical methods of bifurcation theory (e.g., Arnold 1983; Khibnik et al. 1993; Kuznetsov 1995; Levitin 1989). Table 1 contains examples of parameter values (μ, ν) for a fixed $\gamma = 1.5$, corresponding to the eight domains of Fig. 1a, b.

4. Equilibria of the model

4.1. Zero-isoclines

The system (4) has the following zero-isoclines (see Fig. 2)

$$\begin{array}{l} x_\tau = 0 : x = 0 \text{ or } y = (1 - x)/(x - (1 - \nu)), \\ y_\tau = 0\text{: } y = 0 \text{ or } y = (\mu - \gamma)x/\gamma \end{array} \tag{6}$$

So, the system (4) has the equilibria $\boldsymbol{O}(x = 0,\ y = 0)$, $\boldsymbol{A}(x = 1,\ y = 0)$ and $\boldsymbol{B}(x = x^*,\ y = y^*)$, where

$$x^* = 1-\nu(\mu-\gamma)/\mu \text{ and } y^* = (\mu-\gamma)x^*/\gamma = (\mu-\gamma)(\mu-\nu(\mu-\gamma))/(\mu\gamma) \tag{7}$$

The equilibria ***O*** and ***A*** exist for all parameter values.

From the relations (7), we obtain the parameter conditions for which the point ***B*** is in the interior of the first quadrant:

[1] The total number of "connections" between parameters.

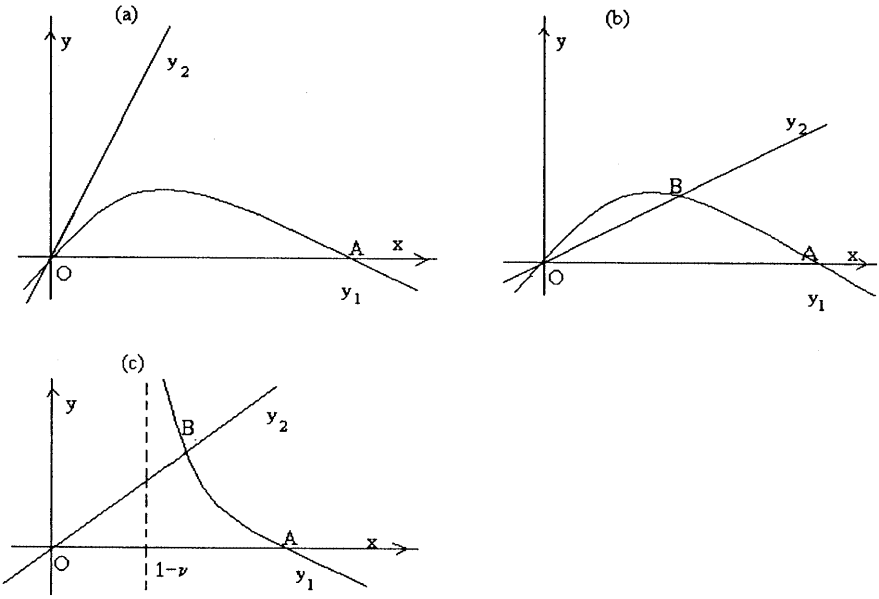

Fig. 2. The three general types of zero-isoclines y_1: $x_\tau = 0$ and y_2: $y_\tau = 0$. The equilibrium points ***O*** and ***A*** exist with all parameter values; the point ***B*** exists if $\mu > \gamma$, $\nu < \mu/(\mu - \gamma)$ (b–c).

$$\mu > \gamma, \nu < \mu/(\mu - \gamma). \tag{8}$$

The equalities $\mu = \gamma$, $\nu = \mu/(\mu - \gamma)$ define parameter surfaces which are boundaries between the different phase behaviors of system (4). In Fig. 1a, both curves ***BA***: $\mu = \gamma$ and ***BO***: $\nu = \mu/(\mu - \gamma)$ correspond to the disappearance of point ***B*** from the first quadrant. Note that in the first case point ***B*** passes into the negative region by merging with point ***A***, whereas in the second case it merges with point ***O*** and disappears. The latter bifurcation has a supplementary degeneracy in the case $\nu = \gamma + 1 = \mu$, that is, at the parametric point α in portrait 1a (this point is discussed below).

*4.2. Complicated equilibrium point **O***

The important mathematical peculiarity of system (4) is that the origin is a *non-analytical complicated equilibrium point*. The structure of a neighborhood of point ***O*** in the first quadrant of the plane (x, y) and the asymptotes of trajectories for $x, y \to 0$ depend on parameter values and can change in an essential way with a change of parameters (Fig. 3).

Lemma 1. *For different positive values of parameters γ, μ, ν, there exist four types of topologically different structures of the neighborhood of point **O** in the first quadrant of the phase plane*:

– *a saddle sector (Fig. 3a) bounded by separatrices $x = 0$ and $y = 0$ for parameter values $0 < \nu < \gamma + 1$, $0 < \mu \leq \gamma + 1$;*

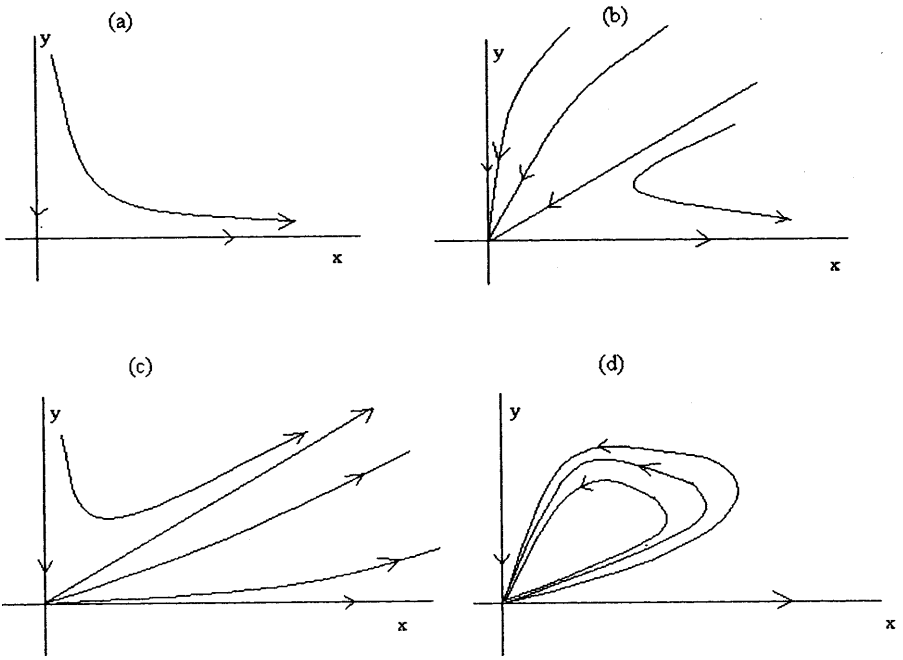

Fig. 3. Structures of a neighborhood of point $\boldsymbol{O}$ in the first quadrant of the plane (x, y): (a) saddle sector for $0 < \nu < \gamma + 1$, $0 < \mu \leq \gamma + 1$; (b) saddle sector and "attracting node" sector for $\gamma + 1 < \nu < \mu/(\mu - \gamma)$, $0 < \mu < \gamma + 1$; (c) saddle sector and "repelling node" sector for $\mu < \gamma + 1$, $0 < \nu < \mu/(\mu - \gamma)$; (d) elliptic sector for $\nu \geq \mu/(\mu - \gamma)$.

– *a saddle sector having the separatrix* $y = 0$ *and an "attracting node" sector* (*containing trajectories tending to 0 with* $t \to \infty$) (*Fig. 3b*) *for parameter values* $\gamma + 1 < \nu < \mu/(\mu - \gamma)$, $0 < \mu < \gamma + 1$;
– *a saddle sector having the separatrix* $x = 0$, *and a "repelling node" sector* (*containing trajectories which originate from* $\boldsymbol{O}$, *i.e. which tend to* $\boldsymbol{O}$ *with* $t \to -\infty$) (*Fig. 3c*) *for parameter values* $\mu < \gamma + 1$, $0 < \nu < \mu/(\mu - \gamma)$;
– *an elliptic sector composed of trajectories tending to* $\boldsymbol{O}$ *with* $t \to \infty$ *as well as with* $t \to -\infty$ (*Fig. 3d*) *for parameter values* $\nu \geq \mu/(\mu - \gamma)$.

The asymptotic behaviors of *characteristic trajectories* (having a definite asymptote for $x, y \to 0$) in the non-degenerate case $(\mu-\gamma-1)(\gamma+1-\nu)(\nu-\mu/(\mu-\gamma)) \neq 0$ are described by Lemma 2. Note that these asymptotes can be curvilinear, they are not necessarily straight lines.

Lemma 2. *If* $\mu \neq \gamma + 1$, $\nu \neq \gamma + 1$, *then each characteristic trajectory of point* $\boldsymbol{O}$ *has an asymptote which belongs to one of the following three types* (*asymptotes of the first two types form parametric families that depend on an arbitrary positive constant* C).

$$\textbf{\textit{Type 1}}\text{: } y = Cx^{\gamma/(\nu-1)}(1 + o(1)), \tag{9}$$

which exists if $\nu > \gamma + 1$ *and corresponds to trajectories tending to point* $\boldsymbol{O}$ *with* $t \to \infty$ (*Fig. 3b and d*);

$$\textbf{\textit{Type}}\ \mathbf{2}\text{: } y = Cx^{\mu-\gamma}(1+o(1)), \tag{10}$$

which exists if $\mu > \gamma + 1$ *and corresponds to trajectories tending to point* ***O*** *with* $t \to -\infty$ (*Fig. 3c and d*).

Finally, the system (4) *has in the positive quadrant one or more trajectories with an asymptote of the third type*

$$\textbf{\textit{Type}}\ \mathbf{3}\text{: } y = Kx(1+o(1)),\ \textit{where}\ K = (\mu-\gamma-1)/(\gamma+1-\nu), \tag{11}$$

which exists if $k > 0$. *The separatrix of point* ***O*** (*see Fig. 3b and c*) *is of the form* (11) *in parameter domains where* $\gamma+1 < \nu < \mu/(\mu-\gamma)$; *the set of characteristic trajectories* (*Fig. 3d*) *is of the form* (11) *in parameter domains* $\nu > \mu/(\mu-\gamma)$, $\gamma < \mu < \gamma+1$ *and* $\mu/(\mu-\gamma) < \nu < \gamma+1$, $\mu > \gamma+1$.

Remark . On the line of the parameter space α: $\nu = +1 = \mu$, the point ***O*** is an equilibrium having an elliptic sector placed in its positive neighborhood and formed by trajectories with asymptotes

$$y = Cx(1+o(1)).$$

The proofs of the Lemmas are in Appendix 1 and use the version of the blow-up method associated with the Newton diagram (Berezovskaya 1976, 1995).

4.3. Equilibrim points ***A*** *and* ***B****. Andronov-Hopf bifurcation*

The Jacobian $\mathbf{J} = (a_{ij})$ $(i, j = 1, 2)$ of system (4) has the following elements:

$$\begin{aligned} a_{11} &\equiv P_x = ((1-x) - \nu y/(x+y)) + (-x + \nu xy/(x+y)^2), \\ a_{12} &\equiv P_y = -\nu x^2/(x+y)^2, \\ a_{21} &\equiv Q_x = \mu y^2/(x+y)^2, \\ a_{22} &\equiv Q_y = -\gamma + \mu x/(x+y) - \mu xy/(x+y)^2. \end{aligned} \tag{12}$$

Calculating the determinant and trace of the Jacobian at the equilibrium points ***A*** and ***B***, we obtain the following results.

At point ***A***, $\det(\mathbf{J}) = -(\mu-\gamma)$, $\mathrm{tr}(\mathbf{J}) = -1 + (\mu-\gamma)$. So, the following statement holds:

Proposition 1. *The point* ***A*** *is a standard saddle if* $\mu > \gamma$ *and a stable node if* $0 < \mu < \gamma$.

It is useful to know the directions of the phase trajectories tending to point ***A***. Due to the system, two of such trajectories are of the form

$$y = 0 \text{ for } x > 1,\ y = 0 \text{ for } 0 < x < 1 \tag{13a}$$

and all other trajectories are of the form:

$$y = k(x-1)(1+o(1)),\ \text{where } k = (\gamma-1-\mu)/\nu \tag{13b}$$

If ***A*** is a saddle, then formulas (13) correspond to its separatrices.

At point $\boldsymbol{B}$, $\det(\mathbf{J}) = \mu\nu x^{*2}y^*/(x^* + y^*)^2 > 0$ if $\boldsymbol{B}$ is in the first quadrant. Therefore $\boldsymbol{B}$ is *a topological node or a focus*. The trace is $\mathrm{tr}(\mathbf{J}) = -x^* + (\nu - \mu)(\mu - \gamma)\gamma/\mu^2$ and the point $\boldsymbol{B}$ is *stable* if $\mathrm{tr}(\mathbf{J}) < 0$ and *unstable* if $\mathrm{tr}(\mathbf{J}) > 0$. It is easy to verify that both cases can occur in the model for appropriate parameter values.

Define now the parametric boundary $\boldsymbol{H}$: $\nu = \mu(\gamma + \mu/(\mu - \gamma))/(\mu + \gamma)$, $\gamma < \mu < \gamma + 1$ which intersects the boundary $\boldsymbol{BO}$ at point α (Fig. 1a). Then $\mathrm{tr}(\mathbf{J}) = 0 \Leftrightarrow \boldsymbol{B} \in \boldsymbol{H}$.

The case $\mathrm{tr}(\mathbf{J}) = 0$ corresponds, in general, to the Andronov-Hopf bifurcation at which the equilibrium point changes its stability with appearance/disappearance of a limit cycle. The stability of this cycle is determined by the first Lyapunov value l_1 (Arnold 1983). By calculating l_1 with the computer package LOCBIF (Khibnik et al. 1993), we showed that l_1 is negative at $\boldsymbol{H}$. So, we have obtained a proof of

Proposition 2. *A supercritical Andronov-Hopf bifurcation of co-dimension* 1 *occurs in system* (4) *on the boundary* $\boldsymbol{H}$.

It follows from this Proposition that crossing $\boldsymbol{H}$ from left to right (for fixed γ, ν) implies a loss of stability of the equilibrium point $\boldsymbol{B}$ and the appearance of a stable limit cycle in the phase plane (Fig. 1a, b).

4.4. Equilibrium points "at infinity"

A complete investigation of the system includes the study of its limit properties at infinitely large values of the variables. We use Poincaré coordinates and study the system behavior in the Poincaré sphere (see Appendix 3).

The result is the following:

Proposition 3. *At the "end" of the* x*-axis* (*when* $x \to \infty$) *the system* (4) *has the equilibrium point* $\boldsymbol{E}_\infty(z \equiv 1/x = 0, u \equiv y/x = 0)$ *which is an unstable node for all values of parameters* (γ, μ, ν).

At the "end" of the y-axis (when $y \to \infty$), the system (4) has the complicated equilibrium point $\boldsymbol{E}^\infty(z \equiv 1/y = 0, w \equiv x/y = 0)$. In the first quadrant of the plane (x, y) this point has only a saddle sector with separatrices $z = 0$ and $w = 0$ if parameter $\nu > 1$, and has two sectors (a saddle sector with separatrix $w = 0$ and a stable node sector) if parameter $0 < \nu < 1$. The surface Inf: $\nu = 1$ separates these two cases in the parameter space (γ, μ, ν).

Complete phase portraits of the system (4) at "infinity" are shown on Fig. 4a, b.

Remark. For values $0 < \nu < 1$, the equilibrium point $\boldsymbol{B}$ exists in the first quadrant (x, y) for all positive values of $\mu > \gamma$.

5. On the limit cycles of the model

In Section 4.3, we have shown that for every fixed γ a stable limit cycle appears at the Andronov-Hopf bifurcation when crossing the parameter boundary $\boldsymbol{H}$ from

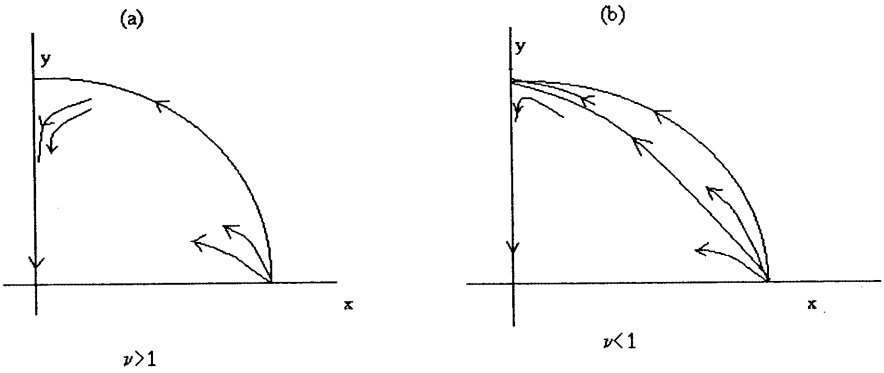

Fig. 4. System behavior "at infinity" of the first quadrant of the plane (x, y), shown on the Poincaré sphere. The point $\boldsymbol{E}_\infty$ (the "end" of the x-axis) is an unstable node for all parameter values, while the point $\boldsymbol{E}^\infty$ (the "end" of the y-axis) is a saddle if $\nu > 1$, and has both a saddle sector and a stable node sector if $0 < \nu < 1$.

the left to the right (see Fig. 1a, b). Such cycle has a small amplitude for parameter values close to the boundary $\boldsymbol{H}$; with a change of parameters the amplitude will grow. For certain parameter values, this cycle was found by computation by Jost et al. (1999). On the other hand, a limit cycle does not exist for parameter values on the right of the boundary $\boldsymbol{BO}$ (because the system has no non-trivial equilibrium points).

So, the parameter boundary on which the limit cycle disappears must be in the "triangular" domain (Fig. 1a) made of the curve $\boldsymbol{H}$, the upper part of $\boldsymbol{BO}$ and the point α: $\nu = \gamma + 1 = \mu$ of their intersection.

We have shown that the cycle appearing at the boundary $\boldsymbol{H}$ grows when the parameter μ increases, whereas the separatrices of the equilibrium points $\boldsymbol{A}$ and $\boldsymbol{O}$ approach each other. For some parameter values, the separatrices of points $\boldsymbol{A}$ and $\boldsymbol{O}$ join in the heteroclinic contour named $\boldsymbol{ao}$ in Fig. 5b. This means that a non-local *heteroclinic bifurcation* occurs in system (4). For these parameter values, the cycle turns into the heteroclinic contour $\boldsymbol{ao}$ and disappears when the separatrices move apart.

The heteroclinic contour $\boldsymbol{ao}$ is formed by the separatrix of the saddle $\boldsymbol{A}$ with an asymptote given by formula (13b), by the separatrix of the complicated point $\boldsymbol{O}$ with an asymptote given by formula (11), together with the equilibrium points $\boldsymbol{A}$ and $\boldsymbol{O}$ and their common separatrix (13a): $y = 0$, $0 < x < 1$. Trajectories with parameter values near this non-local heteroclinic bifurcation are shown on Fig. 5a, c.

Thus the limit cycle that appears at the local Andronov-Hopf bifurcation disappears at the non-local heteroclinic bifurcation. Note that the amplitude and period of the cycle grow with a change of parameters, in such way that the period tends to infinity when the cycle "tends" to the separatrix contour.

Parameter values for which the heteroclinic contour exists define the bifurcation curve $\boldsymbol{L}$ in the plane (μ, ν) which intersects the line $\boldsymbol{BO}$ at the point α: $\nu = \gamma + 1 = \mu$ (see Fig. 1a).

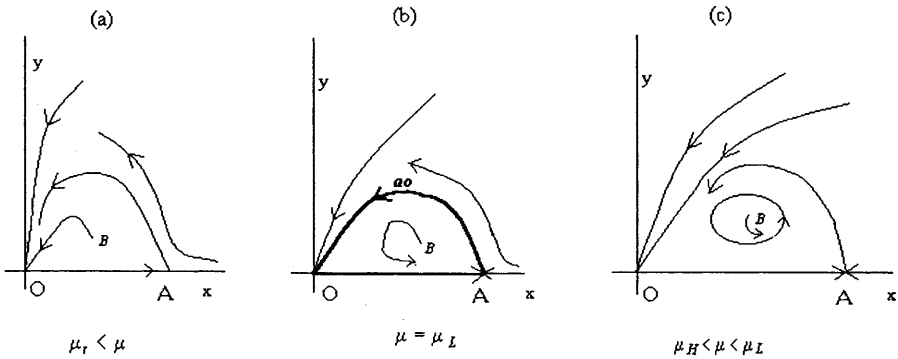

Fig. 5. Behaviors of the model in the plane (x, y) near the non-local heteroclinic bifurcation. (b) "Biangular" heteroclinic contour ***ao*** formed by the points ***A*** and ***O*** together with their joint separatrices; (a, c) the separatrices of the saddle point ***A*** and of the complicated equilibrium point ***O*** interchange their positions relatively to each other.

The respective positioning of the boundaries ***H*** and ***L*** is shown on Fig. 1a and is described by

Proposition 4. *Let* $\nu > \gamma + 1$. *Varying the parameter* μ, *a stable limit cycle appears for parameter values* $(\gamma^*, \nu^*, \mu_{\boldsymbol{H}})$ *corresponding to* ***H***, *and disappears for values* $(\gamma^*, \nu^*, \mu_{\boldsymbol{L}})$ *corresponding to* ***L***, $\mu_{\boldsymbol{L}} > \mu_{\boldsymbol{H}}$.

The proof of Proposition 4 follows directly from its formulation. The proof is also based on Proposition 5. Accounting for structures of the equilibrium points of system (4) (including the structures of the infinite equilibrium points $\boldsymbol{E}_\infty$, $\boldsymbol{E}^\infty$), we show that the heteroclinic contour ***ao*** exists for some parameter values belonging to the domain bounded by the line ***NN*** and the upper parts of line ***BA*** and curve ***BO*** (Fig. 1a), for every fixed value of parameter γ.

Then, we found numerically some parameter points on the bifurcation boundary ***L*** which corresponds to the heteroclinic bifurcation occurring in system (4).

Finally, we analyze the stability of the limit cycle close to the mentioned contour, using Dulac's criterion (Dulac 1923). The following statement holds.

Proposition 5. *A heteroclinic contour* ***ao*** *in the parameter domain* $\gamma + 1 < \nu < \mu/(\mu - \gamma)$, $\gamma < \mu < \gamma + 1$ *formed by the equilibrium points* ***O*** *and* ***A*** *together with their joint separatrices is stable.*

A proof of this proposition is given in Appendix 2.

The most difficult part in the investigation was the computation of the separatrix of the complicated point ***O***. It demands to use blow-up coordinates $(x, u = y/x)$ (see Appendix 1) in which the complicated equilibrium point ***O*** "splits" into two non-degenerated saddles $\boldsymbol{O}_1$, ***K***. The point ***A*** is a saddle too. The contour ***ao*** (see Fig. 5b) is transformed into the "triangular" contour ***aok*** (see Fig. A2b) formed by the separatrices of these three saddles. This heteroclinic contour corresponding to the disappearance of the stable limit cycle was found for some parameter values with help of the package TRAX (Levitin 1989).

Note that the mentioned heteroclinic bifurcation of system (4) has co-dimension 1 whereas, in general, such bifurcation has co-dimension 2 because it requires enclosing *two* pairs of separatrices. In our case, however, one of the contour curves is the trajectory $y = 0$ for $0 < x < 1$, which exists for all parameter values due to the model suppositions[2]. So, this bifurcation occurs on the boundary surface $\boldsymbol{L}$ in the parameter space (γ, μ, ν) (see Fig. 1a).

Proposition 6. *System* (4) *has no other limit cycles in the positive phase plane than those described above.*

The validity of this statement is obvious for parameter values on the right of the boundary ***BO*** and on the left of the boundary ***BA*** (see Fig. 1a) because with these parameter values the system has no nontrivial equilibria. The absence of limit cycles was examined by careful numerical investigations in the parameter domain $\nu < \gamma + 1$ (located below the boundary ***NN*** in Fig. 1a) was proved by Jost et al. (1999). Finally, numerical investigations of the system inside the parameter domains bounded by ***BA***, ***H*** and ***NN*** as well as ***L*** and ***BO*** have shown the absence of cycles there.

6. The end of the theorem proof

The above analysis of system (4) contained in Lemmas 1–2 and Propositions 1–6 gives the possibility to construct the (μ, ν)-portrait for a fixed "typical" value of parameter γ. This portrait consists of 12 parameter domains differing in the topology of the corresponding phase portraits or in the asymptotes of characteristic trajectories.

Note that it follows from the structures of the point ***B*** and the "infinity" points $\boldsymbol{E}_\infty, \boldsymbol{E}^\infty$ (see Proposition 3 and the Remark in Section 4.4), that all main behaviors of system (4) occur only in the finite part of the phase plane (x, y). This allows to disregard rearrangements for infinitely large values of the variables (x, y) concerned with point $\boldsymbol{E}_\infty$.

Note, additionally, that the three phase portraits which are possible for $\nu > \mu/(\mu-\gamma)$ in domain 1 (see Fig. A1) differ only in the asymptotes of the trajectories and are identical topologically.

Therefore, the bifurcation portrait of system (4) has the form shown on Figs. 1a, 1b.

7. Interpretation of phase and parameter portraits

Let us give an ecological interpretation of the various behaviors of the ratio-dependent predator–prey system (4), in response to changes of the following ecological parameters: the consumption ability ν, the predator growing ability μ, and the predator death rate γ. We shall essentially use the bifurcation diagram given by Figs. 1a and 1b. It demonstrates eight types of system dynamics according to values of ν and μ for a fixed value of γ.

[2] The same property is typical for many modifications of the Lotka-Volterra model (see Bazykin 1985, 1998).

The fundamental paradigm of theoretical ecology is that any "real" prey-predator system can exist only with parameter values providing "stable regimes", such as steady states (Fig. 1b, portraits 2, 3, 4) or stable oscillations (Fig. 1b, portrait 5). Changes of parameter values (caused by changes of environmental conditions or other reasons) can lead the system into parametric domains where one or both populations go extinct in different ways. Our analysis permits to describe completely the parametric domains of stable coexistence and to predict what can occur if the system gets out of these domains.

There exist three main intervals of the predator growing ability μ: $0 < \mu < \gamma$, $\gamma < \mu < \gamma + 1$ and $\mu > \gamma + 1$ that correspond to distinct system behaviors.

7.1. Small predator growing ability: $0 < \mu < \gamma$

Then, for any ν, the system belongs to domains 7 or 8 of the parameter portrait (Fig. 1a). The respective phase portraits given in Fig. 1b exhibit extinction of the predator population y in both domains 7 and 8 (because $\boldsymbol{O}(x^* = 0, y^* = 0)$, $\boldsymbol{A}(x^* = 1, y^* = 0)$ are the only steady states). Predators are unable to reproduce fast enough to compensate their death rate γ. Whatever the amount of prey consumed, this food does not allow them to reproduce fast enough. Such predators are "*maladapted to the prey*".

Note an essential difference between domains 7 and 8. Within the domain 8 ($\nu < \gamma + 1$), the consumption ability ν is low and as a result the prey population survives. Within the domain 7 ($\nu > \gamma + 1$), the consumption ability ν is high enough that predators can drive both populations to extinction. This occurs only in a given region of initial conditions (Fig. 1b, portrait 7).

7.2. Intermediate predator growing ability: $\gamma < \mu < \gamma + 1$

This corresponds to the domains 3, 4, 5, and 6. If the consumption ability is not very large (domain 3: $0 < \nu < \gamma + 1$), then both prey and predator populations coexist at the steady state $\boldsymbol{B}(\boldsymbol{x}^* = 1 - \nu(\mu - \gamma)/\mu, \boldsymbol{y}^* = (\mu - \gamma)(\mu - \nu(\mu - \gamma))/(\mu\gamma))$. Here, the consumption ability and growing ability generate balanced dynamics of both populations. Note that such behavior has also been described by several predator–prey models incorporating the familiar logistic form of prey growth rate and prey-dependent trophic functions like Lotka-Volterra or Holling functions (see, e.g., Bazykin 1998, #3.3.1, #3.4.1).

The peculiarities of our model are revealed more clearly if predators are more active (domains 4, 5, 6: $\nu > \gamma + 1$). In domain 4 (Fig. 1a) populations reach either coexistence or co-extinction *depending on their initial conditions* (Fig. 1b, portrait 4). Further, from domain 4, the system enters domain 5 with the growth of either parameter ν or μ. The coexisting regime is now a stable limit cycle but, depending on initial conditions, co-extinction can occur as in domain 5. With further growth of parameters ν or μ, the system can enter domain 6 in which both populations go extinct from any initial values.

Let us consider in more detail the peculiarities of system dynamics in domains 4 and 5. We have shown (Lemma 2) that "extinction trajectories" form a family of

curves having the phase asymptotes (9). The separatrix of the complicated point ***O*** has the asymptote (11).

Note first that, for fixed γ, μ, ν, a system with large initial abundances can become extinct while the same system with low initial abundances can survive; the result depends mainly on *the ratio of prey and predator initial numbers*. This outcome follows from the "linearity" of the separatrix asymptote (11) for small values of x, y and was confirmed by numerous computer simulations for initial values which were not small. Note further that, for fixed $\mu < \gamma + 1$, the exponent of asymptotes (9) decreases when ν increases. This means that predators go extinct faster than the prey, under growing consumption ability ν. The tangent K of separatrix (11) decreases when either ν or μ increases. Thus, the area of initial values for which populations reach coexistence becomes smaller. This area vanishes when the parametric point (μ, ν) enters the parametric domain 6.

Thus, we have proved that the ratio-dependent model (4) demonstrates in the domains 4, 5, and 6 of parameter space a unique behavior that distinguishes it from standard prey-dependent predator–prey models (see Introduction). In these domains, the origin ***O*** possesses its own basin of attraction. The existence of such region of co-extinction was foreseen by Arditi and Ginzburg (1989) with the isocline method, its ecological basis was discussed by Akçakaya et al. (1995) and it was also proved by Jost et al. (1999).

7.3. High predator growing ability: $\mu > \gamma + 1$

Two different situations are possible here (domains 1 and 2 in Fig. 1a).

Domain 1 corresponds to the condition $\nu > \mu/(\mu - \gamma)$ and both populations go to extinction from any initial abundance. The following interpretation can be made. Due to the high consumption ability and the high predator growing ability (compared with the death rate), the predator population increases so quickly that all prey are consumed. Such predators are "*overly efficient*."

It is interesting that, under this condition, there exist two different types of extinction trajectories (Fig. 1b, portrait 1). The first one corresponds to the elliptic sector (Fig. 3d): the trajectories approach the origin in both forward and reverse time ($t \to \pm\infty$). This means that for *arbitrary* small initial values of abundance, both populations begin to grow for some time and after a certain period begin to decrease and become extinct simultaneously. The other extinction trajectories belong to a the region above the separatrix (13b) of point ***A*** possessing the asymptote $y = k(x - 1)(1 + o(1))$, where $k = (\gamma - 1 - \mu)/\nu$. For these trajectories, the number of prey decrease monotonically when $t \to \infty$.

It is now possible to answer one of the first arguments that was raised against ratio dependence in predator–prey models. Under certain conditions, the model can predict that both variables get "arbitrarily close to the axes" (Freedman and Mathsen 1993), which was considered as "pathological" in a mathematical sense. In biological terms this "pathological" dynamics means that both populations increase initially, then predators consume all the prey and both populations go extinct. This is quite a reasonable outcome for biologists, as it was demonstrated by Gause's experiments (see Akçakaya et al. 1995). It is easy to see that this dynamics corre-

sponds exactly to the "elliptic" trajectories (Fig. 3d). Our analytical investigation has proved that the elliptic sector is realized in the model with all parameter values belonging to domain 1; the asymptotes of these trajectories are given by formulas (9–11). Changes of the elliptic trajectories are caused by changes of the model parameters.

Consider now domain 2, characterized by $\nu < \mu/(\mu - \gamma)$. Here, prey and predators coexist in a steady state for any initial numbers (Fig. 1b, portrait 2). So, the threshold $\nu = \mu/(\mu - \gamma)$ of the consumption ability is of a critical importance for system coexistence.

Let's now compare the system behavior characteristics in domain 2 with those in the neighboring domain 3. In the phase portrait 2, a positive neighborhood of the origin consists of two sectors: a "saddle" sector and an "unstable node" sector, which are separated by the separatrix (11) (Fig. 3c). The node sector has trajectories with asymptotes (10). These trajectories make both populations grow to the equilibrium $\boldsymbol{B}(x^* = 1 - \nu + \nu\gamma/\mu,\ y^* = (\mu - \gamma)x^*/\gamma)$. Note that with $\nu \leq 1$, the steady state $\boldsymbol{B}$ exists for any arbitrarily large $\mu > \gamma$. Note that for a fixed consumption ability ν, an increase of the growing ability μ leads to a decrease of x^* together with an increase of y^*. So, for a fixed ν, with parameter values belonging to domain 2, the equilibrium x^* is lower and the equilibrium y^* is higher than the corresponding numbers in domain 3.

With changes of parameters, the point (μ, ν) can move from domain 2 either to domain 3 or to domain 1 (see Fig. 1a). In the first case, crossing the boundary ***MM*** does not change crucial qualitative characteristics of system behavior whereas, in the second case, crossing the boundary ***BO*** results in extinction of both populations.

Finally, it is relevant to discuss one more peculiarity of the model. Usually, in predator–prey models, the predator growing ability μ is assumed to be less than the consumption ability ν. This follows from the supposition that the prey x is the only food of the predators y. Remark that all above types of system behavior (except domain 2) are realized for parameter values $\mu \leq \nu$. However, the parametric domain $\mu \geq \nu$ can be of interest as well. For example, this is the case when predators y feed on other resources in such a way that the prey x is the limiting factor. According to Liebig's principle of limiting factors, the growing ability μ should be proportional to $\min\{a\nu, b\rho\}$, where ρ is the consumption ability on other resources and a, b are "stoechiometric factors" (Poletaev 1966). For such parameter values with $\mu \geq \nu$, the system must belong to domains 2, 3 or 1. In particular, the system can coexist steadily under $\nu \leq 1$ with arbitrary large $\mu > \gamma$.

8. Summarized conditions of coexistence and extinction

Populations of predators and prey reach a steady state of coexistence for any initial densities in both domains 2 and 3 (Fig. 1). The difference in system dynamics is revealed only for small values of predator numbers because the system is restored more quickly in domain 2 than in domain 3. We can consider that the boundary ***MM*** which divides these two domains is "soft" (meaning that no new steady states or other attractors appear when crossing this boundary) and we can roughly pool domains 2 and 3 into a common "*area of unconditional population coexistence*".

Depending on initial conditions, populations of predators and prey either coexist or get extinct in both domains 4 and 5. This important characteristic of system dynamics suggests to pool these two domains into a unique "*area of conditional population coexistence*", the difference being that in domain 4 the populations coexist in a steady regime whereas in domain 5 they coexist on a limit cycle. Again, the boundary ***H*** between the domains 4 and 5 is "soft", since the system's behavior does not change in an essential way when crossing it.

Populations of predators and prey become extinct both in domain 6 (with oscillations) and in domain 1. So, the boundary between these domains, represented by the upper part of curve ***BO*** in Fig. 1a, is "soft" too. We can pool domains 1 and 6 into an "*area of unconditional population extinction*".

Thus, after pooling domains of Fig. 1a from the point of view of coexistence or extinction of populations, we obtain the simpler diagram of Fig. 6. It contains only five areas of parameters (γ, μ, ν), corresponding to qualitatively different dynamics of the system.

- In Area I (union of domains 1 and 6), both populations go extinct for any initial values.
- In Area II (union of domains 2 and 3), both populations coexist for any initial values.
- In Area III (union of domains 4 and 5), populations reach either coexistence or co-extinction depending on the initial values.

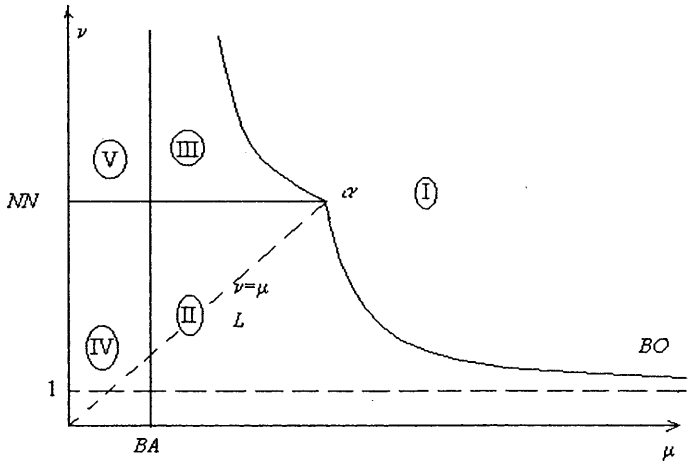

Fig. 6. Simplified parameter portrait regarding coexistence and extinction. Area I: both populations go extinct for all initial values; Area II: both populations coexist for all initial values; Area III: populations reach either coexistence or extinction depending on their initial values; Areas IV and V: the predator population becomes extinct for all initial values, the prey population always survives in Area IV, while it can become extinct for some initial values in Area V. The parameter domain $\mu \leq \nu$ corresponds to a situation in which the prey x are the only food of predators y. The parametric domain $\mu \geq \nu$ corresponds to the case in which predators y also feed on other resources than the prey x, and in which x is a "limiting factor" for the growth of y.

– Area IV is identical to domain 8 and Area V is identical to domain 7. In both cases, the predator population becomes extinct from all initial values. In Area IV, the prey population always survives while in Area V, it can become extinct for some initial values, in an analogous way to Areas II and III.

Area I has the boundary ***BO*** with Area II and the boundary ***L*** with Area III. Crossing these boundaries into Area I leads to extinction of both populations. Areas II and IV as well as Areas III and V have the common boundary ***BA***. Crossing this boundary from right to left leads to extinction of the predator population only. Note that Area I has no common boundary with Areas IV and V. This means that a transition from an area of predator extinction into an area of extinction of both populations is only possible through an area of coexistence (Areas II or III).

In more biological terms, Areas IV and V correspond to predators that reproduce very inefficiently, unable to survive even with plenty of prey (see phase portraits 8 and 7 in Fig. 1b). This normally leads the prey to reach its carrying capacity. [An exception can occur in Area V, in the unusual case that the predators are very efficient consumers and very inefficient reproducers: in this case the prey can be led to extinction for unfavorable initial conditions.] With more efficiently reproducing predators, the system enters Areas II and III (phase portraits 2, 3, 4, and 5 of Fig. 1b). This permits coexistence unless (in Area III) the predators are "disproportionately" efficient consumers that can lead the prey to extinction if their initial values are unfavorable. Finally, very efficient predators (both in terms of consumption and reproduction) place the system in Area I (see phase portraits 1 and 6 of Fig. 1b). There, the predators always drive the prey to extinction and, consequently, become extinct themselves.

As already explained in the Introduction, all these dynamic behaviors have been observed in real populations but prey-dependent models are not able to produce them all. Particularly, the ratio-dependent model is able to reproduce the fact that extinction or coexistence can depend on the initial conditions (e.g., Huffaker 1958, Luckinbill 1973). This occurs in Areas III and V.

From the perspective of biological control, for which prey (=pest) extinction is desirable, Area I is the most interesting. In this case, both populations are driven to extinction deterministically, an outcome that prey-dependent models are unable to produce. If some stochasticity is considered for low abundance values, the extinction can be accompanied by oscillations (see phase portrait 1 of Fig. 1b). Quite naturally, this is obtained with efficient predators (high values of ν and/or μ). Note that in classical prey-dependent models, biological control is impossible to achieve because efficient predators lead to huge limit cycles (see Arditi and Berryman 1991).

From the perspective of biological conservation, for which coexistence is desirable, Areas II and III are those that must be maintained. The boundaries of these two areas can be considered "dangerous" because one or both populations become extinct when crossing them. When they are approached, one can observe:

– an increase of the period of oscillations when approaching the boundary ***L*** (in Area III),
– a decline of the prey steady state when approaching the boundary ***BO*** (in Area II),

– a decline of the predator steady state when approaching the boundary ***BA*** (in Areas II or III).

If these phenomena are observed in biological populations, this can be interpreted as signs that the system is approaching dangerous conditions. Assuming that the endangered species is the predator, extinction can occur for two reasons: if the growing ability μ declines for some reason (e.g., because of habitat fragmentation leading to energy losses), the system can cross the boundary ***BA*** and enter Areas IV or V. Conversely, if the predator becomes very efficient at capturing food (e.g., because the prey becomes vulnerable) or if its growing ability increases (e.g., because of increased temperature), the system can enter the situation of biological control (see above) and become extinct because of prey over-exploitation.

Appendix 1. Complicated equilibrium point *O*. Proof of Lemmas 1 and 2

System (4) is analytical in all points of the plane (x, y) except the origin. The positioning of its phase trajectories in the first quadrant is identical to those of the polynomial system

$$\begin{aligned} x_\tau &= x(1-x)(x+y) - \nu xy = x^2 + (1-\nu)xy - x^2(x+y) \\ y_\tau &= -\gamma y(x+y) + \mu xy = (\mu-\gamma)xy - \gamma y^2 \end{aligned} \tag{A.1}$$

obtained from (4) by a change of the independent variable:

$$dt = (x+y)d\tau \tag{A.2}$$

System (A.1) has a complicated equilibrium point at the origin (because both eigenvalues are equal to zero) which is investigated below by methods developed in [Berezovskaya 1976, 1995; Berezovskaya and Medvedeva 1994]. It follows from these results that, if $\nu \neq \mu/(\mu-\gamma)$, the homogeneous system

$$\begin{aligned} x_\tau &= x^2 + (1-\nu)xy \\ y_\tau &= (\mu-\gamma)xy - \gamma y^2 \end{aligned} \tag{A.3}$$

is the main part of system (A.1) in a neighborhood of point ***O*** and provides also the asymptotes of its characteristic trajectories. So, for describing the behavior of system (A.1) in a neighborhood of the origin, we can integrate the homogeneous system (A.3). However, as we are not only interested in a "small" neighborhood of point ***O***, we make a blow-up procedure for the complete system (A.2).

The first step consists in a change of variables in system (A.1) [see also Jost et al. 1999]:

$$\begin{gathered} x = x,\ u = y/x \\ d\tau = x^2\, ds \end{gathered} \tag{A.4}$$

that transforms in a non-degenerate way the first quadrant of the (x, y)-plane, except $x = 0$, into the first quadrant of the (x, u)-plane and blows-up the point ***O*** into the u-axis.

We obtain the system

$$\begin{aligned} x_s &= x(1+(1-\nu)u - x(1+u)) \\ u_s &= -(\gamma+1-\nu)u^2 + (\mu-\gamma-1)u + ux(1+u) \end{aligned} \tag{A.5}$$

which has two equilibrium points on the u-axis: $\boldsymbol{O}_1(0,0)$ and $\boldsymbol{K}(0,k)$ with $k = (\mu-\gamma-1)/(\gamma+1-\nu)$. The eigenvalues of these points are:

$$\begin{gathered} \boldsymbol{O}_1\colon \lambda_1(\boldsymbol{O}_1) = 1,\ \lambda_2(\boldsymbol{O}_1) = \mu-\gamma-1, \\ \boldsymbol{K}\colon \lambda_1(\boldsymbol{K}) = -(\mu-\gamma-1),\ \lambda_2(\boldsymbol{K}) = (\mu-\nu(\mu-\gamma))/(\gamma+1-\nu) \end{gathered} \tag{A.6}$$

So, both points are non-degenerate if $(\gamma+1-\nu)(\mu-\gamma-1)(\mu-\nu(\mu-\gamma)) \neq 0$. Depending on the parameters γ, μ, ν the following cases are realized in the system (A.5) in the first quadrant of the (x,u)-plane (Fig. A1):

(1) single saddle $\boldsymbol{O}_1$ if $\mu < \gamma+1$ and $\nu < \gamma+1$;
(2) single unstable node $\boldsymbol{O}_1$ if $\mu > \gamma+1$ and $\nu > \gamma+1$;
(3) saddle $\boldsymbol{O}_1$ and saddle $\boldsymbol{K}$ if $\gamma < \mu < \gamma+1$ and $\gamma+1 < \nu < \mu/(\mu-\gamma)$ or if $\mu < \gamma$ and $\nu > \gamma+1$;
(4) saddle $\boldsymbol{O}_1$ and unstable node $\boldsymbol{K}$ if $\mu < \gamma+1$ and $\nu > \mu/(\mu-\gamma)$;
(5) unstable node $\boldsymbol{O}_1$ and saddle $\boldsymbol{K}$ if $\mu > \gamma+1$ and $\nu < \mu/(\mu-\gamma)$;
(6) unstable node $\boldsymbol{O}_1$ and stable node $\boldsymbol{K}$ if $\mu > \gamma+1$ and $\mu/(\mu-\gamma) < \nu < \gamma+1$.

We now repeat the blow-up procedure to study the behavior of the system close to the y-axes:

$$\begin{gathered} y = y,\ w = x/y \\ d\tau = y^2\, ds \end{gathered} \tag{A.7}$$

This transformation is non-degenerate for all values of x, y except $y = 0$ and the point $\boldsymbol{O}$ blows-up into the w-axes. In variables (w, y) we obtain the system

$$\begin{aligned} w_s &= (\gamma+1-\mu)w^2 + (\gamma+1-\nu)w - yw^2(w+1) \\ y_s &= y(-\gamma + (\mu-\gamma)w) \end{aligned} \tag{A.8}$$

which has on the w-axis the equilibria $\boldsymbol{O}_1^*(0,0)$ and $\boldsymbol{K}^*(k^*,0)$ with $k^* = (\gamma+1-\nu)/(\mu-\gamma-1)$. Point $\boldsymbol{O}_1^*$ is new (it was not seen in the map (x,u)) whereas point $\boldsymbol{K}^*$ corresponds to point $\boldsymbol{K}$ and we do not need to study it again.

The eigenvalues of point $\boldsymbol{O}_1^*$ are:

$$\lambda_1(\boldsymbol{O}_1^*) = -\gamma,\ \lambda_2(\boldsymbol{O}_1^*) = 1-\nu+\gamma \tag{A.9}$$

So, point $\boldsymbol{O}_1^*$ is a saddle if $\nu < \gamma+1$ and a stable node if $\nu > \gamma+1$ (see Fig. A1).

Assembling together the obtained results and returning to the initial variables (x, y) as shown in Fig. A1, we obtain different topological structures of the complicated point $\boldsymbol{O}$ in the first quadrant of the plane (x, y) depending on system parameters.

Note now that the three types of phase portraits of point $\boldsymbol{O}$ presented on Fig. A1 for $\nu > \mu/(\mu-\gamma)$ are topologically equivalent and differ only in the asymptotes

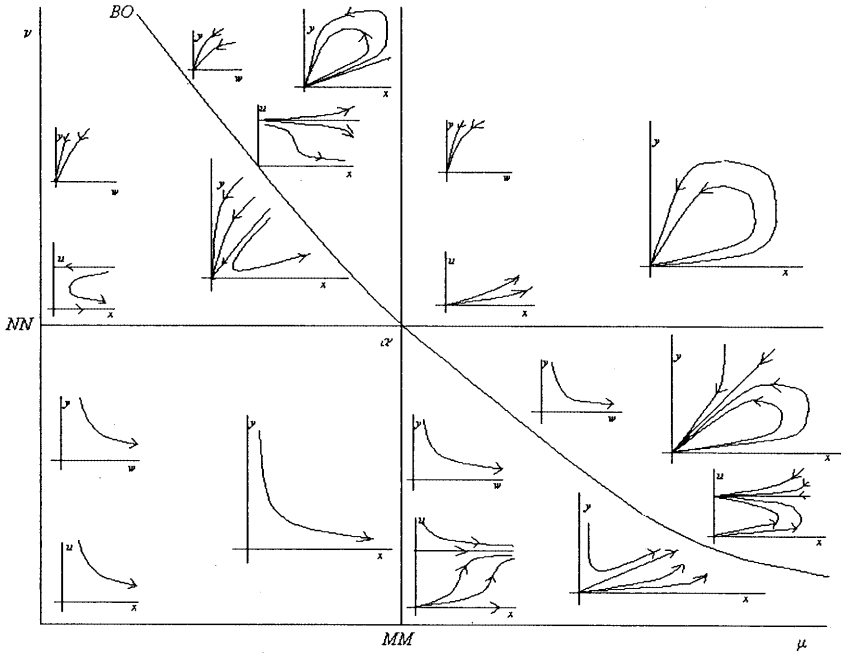

Fig. A1. Six qualitatively or asymptotically distinct structures of the phase curves in a positive neighborhood of the point α [obtained by the blow-up procedures ($x = x, u = y/x$) and ($y = y, w = x/y$) applied to model (4)].

of characteristic trajectories. They should be pooled together in the "unified" phase portrait. Therefore, there are only four topologically different structures in the plane (x, y) in non-degenerate cases; they are presented in Fig. 3.

At the parameter boundary ***MM***: $\mu = \gamma + 1$, $\nu < \gamma + 1$, system (A.5) has the saddle-node $\boldsymbol{O}_1$ with a repelling node sector; at the parameter boundary ***NN***: $\nu = \gamma + 1$, $\mu < \gamma + 1$ system (A.8) has the saddle-node $\boldsymbol{O}_1^*$ with an attracting node sector. In both cases, only the saddle sector is situated in the positive quadrant.

At the parameter boundary ***BO***: $\nu = \mu/(\mu - \gamma)$ the point $\boldsymbol{O}$ has an elliptic sector in its positive neighborhood. Note that the study of the case corresponding to this boundary has demanded to repeat the blow-up procedure for the point $\boldsymbol{K}$ of system (A.5) (or point $\boldsymbol{K}^*$ of system (A.8)).

Proof of Lemma 1 is now complete.

The above analysis gives the possibility to show the asymptotes of trajectories which tend to point $\boldsymbol{O}$ and, thereby, prove Lemma 2.

Point $\boldsymbol{O}_1$ of system (A.5) can only be an *unstable* one. If it is an unstable node ($\mu > \gamma + 1$), then in the plane $(x, u)\boldsymbol{O_1}$ is the source of a family of trajectories with asymptotes

$$u = Cx^{\mu-\gamma-1}(1 + o(1)) \text{ (where } C \text{ is an arbitrary constant).}$$

In coordinates (x, y) this family is transformed into *Family* 2 (see Section 4.2).

If point $\boldsymbol{O}_1^*$ is a *stable* node of system (A.8) (for $\nu > \gamma + 1$), it is reached in the plane (w, y) by a family of trajectories with asymptotes

$$w = Cy^{(\gamma/(\nu-1))-1}(1 + o(1)) \text{ (where } C \text{ is arbitrary constant)}.$$

In coordinates (x, y) this family is transformed into *Family* 1 (see Section 4.2).

Finally, point $\boldsymbol{K}(k, 0)$ with $k = (\mu - \gamma - 1)/(\gamma + 1 - \nu)$ in system (A.5) can have different topological type depending on parameters: *a saddle*, *a stable* or *an unstable node*.

If $\boldsymbol{K}$ is a saddle (for $0 < \mu < \gamma + 1$ and $\gamma + 1 < \nu < \mu/(\mu - \gamma)$ or $\mu > \gamma + 1$ and $\nu < \gamma + 1$), then the curve $u = k(1 + o(1))$ is the asymptote of the separatrix. Therefore the curve

$$\boldsymbol{s}\text{: } y = kx(1 + o(1))$$

is a separatrix of the saddle sector of point $\boldsymbol{O}$ in the plane (x, y).

If $\boldsymbol{K}$ is a stable/unstable node, then a set of trajectories which lie in an attracting/repelling sector in a positive neighborhood of point $\boldsymbol{O}$, have the same asymptote with a positive value of k (see Fig. A2).

This completes the investigation of point $\boldsymbol{O}$ in cases of non-degeneracy.

If $\mu = \gamma + 1$, $\nu \neq \gamma + 1$, then point $\boldsymbol{O}_1$ of system (A.5) is a saddle-node; its characteristic trajectories have asymptotes that can be easily obtained by integrating system (A.5) in a neighborhood of point $\boldsymbol{O}_1$. In coordinates (x, y), we obtain the family of trajectories:

$$y = (\gamma + 1 - \nu)x/\ln(Cx)\ (1 + o(1)).$$

We can treat analogously the point $\boldsymbol{O}_1^*$ of system (A.8) with $\nu = \gamma + 1$, $\mu \neq \gamma + 1$. In coordinates (x, y) we obtain the family of trajectories:

$$x = (\gamma/(\mu - \gamma - 1)y\ \ln(Cy)\ (1 + o(1)),$$

C being an arbitrary constant in both cases.

Finally, if $\nu = \gamma + 1 = \mu$ then system (A.8) can be reduced to the equation:

$$dw/dy = w^2(w + 1)/(\gamma - w).$$

The integral of this equation in variables (x, y) has the form given by formula (5). Note that the point $\boldsymbol{O}$ possesses an elliptic sector in the first quadrant of the plane (x, y).

Appendix 2. Stability of the heteroclinic cycle. Proof of Proposition 5

The cycle considered appears from the contour $\boldsymbol{ao}$ formed by the separatrices of the saddle point $\boldsymbol{A}$ and the complicated equilibrium $\boldsymbol{O}$ of system (A.1); it contains the point $\boldsymbol{B}$ inside itself (see Fig. 5b).

In the parameter domain $\gamma + 1 < \nu < \mu/(\mu - \gamma)$, $\gamma < \mu < \gamma + 1$, the blow-up (A4) "splits" point $\boldsymbol{O}$ into the saddles $\boldsymbol{O}_1(0, 0)$ and $\boldsymbol{K}(0, k)$ with $k =$

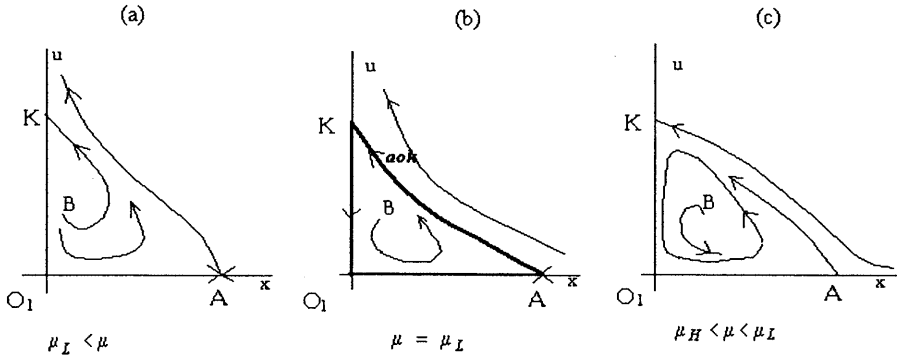

Fig. A2. Behavior of the model in the plane $(x, u = y/x)$ near the non-local heteroclinic bifurcation. Equilibrium points $\boldsymbol{O}_1$, $\boldsymbol{A}$ and $\boldsymbol{K}$ are saddles. (b) the "triangular" heteroclinic contour ***aok*** formed by the saddles $\boldsymbol{A}$, $\boldsymbol{O}_1$ and $\boldsymbol{K}$ together with their joint separatrices; (a, c) the separatrices of the saddles $\boldsymbol{A}$ and $\boldsymbol{K}$ interchange their positions relatively to each other.

$(\mu-\gamma-1)/(\gamma+1-\nu)$ (see Appendix 1) retains point $\boldsymbol{A}$ and transforms heteroclinics ***ao*** into heteroclinics ***aok*** containing point $\boldsymbol{B}$ inside itself (see Fig. A2b).

Finding the parameter values for which separatrices coincide is a problem that can be solved, in general, only by computation. On the contrary, the stability of the cycle that appears by heteroclinic bifurcation can be estimated with help of a simple local condition, namely by the ratio of the eigenvalues of the system at the saddles forming the contour, and given by Dulac criterion (Dulac 1923)[3].

We use this criterion to prove stability of the heteroclinic contour ***aok*** of system (A.5) in the plane (x, u). After this, returning to the variables (x, y), we obtain that the heteroclinic contour ***ao*** of system (4) is stable (see Figs. 2a and 5).

It is easy to calculate from the Jacobian of system (A.5) (see Eqs. A.6) that in the considered parameter domain the positive (λ^+) and negative (λ^-) eigenvalues are of the form:

$$\lambda^+(\boldsymbol{O}_1) = 1,\ \lambda^-(\boldsymbol{O}_1) = \mu - \gamma - 1;$$
$$\lambda^+(\boldsymbol{K}) = -(\mu - \gamma - 1),\ \lambda^-(\boldsymbol{K}) = (\mu - \nu(\mu - \gamma))/(\gamma + 1 - \nu) < \gamma + 1;$$
$$\lambda^+(\boldsymbol{A}) = (\mu - \gamma),\ \lambda^-(\boldsymbol{A}) = -1.$$

The value

$$S = \left|\lambda^+(\boldsymbol{O}_1)\lambda^+(\boldsymbol{K})\lambda^+(\boldsymbol{A})/(\lambda^-(\boldsymbol{O}_1)\lambda^-(\boldsymbol{K})\lambda^-(\boldsymbol{A}))\right| - 1 < 0$$

Therefore, the heteroclinic cycle of system (A.5) must be stable. Returning to system (4), we obtain that a cycle close to the contour ***ao*** should be stable.

[3] Let $\lambda^+(\boldsymbol{O}_1)$, $\lambda^+(\boldsymbol{O}_2), \ldots, \lambda^+(\boldsymbol{O}_n)$ be the positive eigenvalues and $\lambda^-(\boldsymbol{O}_1)$, $\lambda^-(\boldsymbol{O}_2), \ldots, \lambda^-(\boldsymbol{O}_n)$ the negative eigenvalues of n non-degenerate saddles $\boldsymbol{O}_1, \boldsymbol{O}_2, \ldots, \boldsymbol{O}_n$, whose separatrices compose the heteroclinic contour. A cycle that appears from this contour is stable if the value $S = |\lambda^+(\boldsymbol{O}_1)\lambda^+(\boldsymbol{O}_2)\ldots\lambda^+(\boldsymbol{O}_n)/\lambda^-(\boldsymbol{O}_1)\lambda^-(\boldsymbol{O}_2)\ldots\lambda^-(\boldsymbol{O}_n)| - 1 < 0$ and unstable if $S > 0$.

Appendix 3. Analysis of system behavior "at infinity"

Let us, at first, study system (4) in the case $x \to \infty$.
The Poincaré map

$$x = 1/z,\ y = u/z$$

applied to system (A.1), which is equivalent to system (4), leads to the system:

$$\begin{aligned} z_t &= (1 + u - z - (1 - \nu)uz)/z \\ u_t &= u(u + 1 + (\mu - \gamma - 1)z - (\gamma + 1 - \nu)uz)/z^2 \end{aligned}$$

By a standard change of the independent variable $d\tau = dt/z^2$, this system is transformed to the equivalent form:

$$\begin{aligned} z_\tau &= z(1 + u - z - (1 - \nu)uz) \\ u_\tau &= u(u + 1 + (\mu - \gamma - 1)z - (\gamma + 1 - \nu)uz) \end{aligned} \tag{A.10}$$

It is easy to see that system (A.10) has the equilibrium point $\boldsymbol{E}_\infty(z = 0, u = 0)$ which is an *unstable node* for all values of parameters (γ, μ, ν).

An analogous procedure is applied to system (4) for the case $y \to \infty$. Changing the variables

$$y = 1/z,\ x = w/z$$

together with a change of the independent variable $d\tau = dt/z^2$ applied to system (A.1) leads to the system:

$$\begin{aligned} z_\tau &= z^2(\gamma - (\mu - \gamma)w) \\ w_\tau &= -w^2(w + 1) + (1 - \nu + \gamma)zw + (1 + \gamma - \mu)zw^2 \end{aligned} \tag{A.11}$$

System (A.11) has the complicated equilibrium point $\boldsymbol{E}_\infty(z = 0, w = 0)$. The analysis of this point by the above-mentioned blow-up method gives the following result.

The complicated point $\boldsymbol{E}_\infty$ in the first quadrant has only one *saddle sector* with separatrices $z = 0$, $w = 0$ if $\nu > 1$ and has two sectors, *a saddle* and *a stable-node*, if $0 < \nu < 1$.

Complete phase portraits of system (4) "at infinity" are shown in Fig. 4a, b.

Appendix 4. On the reduction of model (1)

In the paper by Jost et al. (1999), the model (1) was reduced with the changes

$$N = A_1 x_1,\ P = B_1 y_1,\ t = C_1 \tau_1, \tag{A.12}$$

with $A_1 = eK/(\alpha h)$, $B_1 = e^2 K/(\alpha h)$, $C_1 = h/e$, setting the parameters to $R = rh/e$, $D = \alpha h/e$ and $Q = qh/e$, and got the form:

$$\begin{aligned} dx_1/d\tau_1 &= Rx_1(1 - x_1/D) - Dx_1 y_1/(y_1 + Dx_1) \\ dy_1/d\tau_1 &= Dx_1 y_1/(y_1 + Dx_1) - Qy_1 \end{aligned} \tag{A.13}$$

In Section 2, model (1) was reduced with different changes of variables and parameters (2–4). It is easy to see the correspondences between parameters and variables of (A.13) and those of (2–4):

$$x/x_1 = 1/D = \mu/\nu,\ y/y_1 = 1/D^2 = (\mu/\nu)^2, \tau/\tau_1 = R = 1/\mu;$$
$$\mu = 1/R,\ \nu = \mu D = D/R,\ \gamma = Q/R.$$

So, both forms (A.13) and (4) of model (1) are equivalent mathematically if parameters are nonzero. This gives the possibility to use results obtained by Jost et al. (1999). For example, it was proved by calculation there that limit cycles are absent under the condition: $D < Q + R \Leftrightarrow \nu < \gamma + 1$ for $\mu \neq 0$.

Acknowledgements. Studies of F. Berezovskaya were supported by grants RFFI N 98-01-00483 and 99-04-49450. G. Karev was holding a visiting position at French CNRS. R. Arditi benefited from a grant of the CNRS program "Modélisation et simulation numérique". This work is a contribution of the French COREV research group.

References

Abrams, P.A.: The fallacies of "ratio-dependent" predation. Ecology, **75**, 1842–1850 (1994)

Abrams, P.A., Ginzburg, L.R.: The nature of predation: prey dependent, ratio dependent or neither? Trends Ecol. Evol., **15**, 337–341 (2000)

Akçakaya, H.R., Arditi, R., Ginzburg, L.R.: Ratio-dependent predation: an abstraction that works, Ecology, **76**, 995–1004 (1995)

Arditi, R., Berryman, A.A.: The biological control paradox. Trends Ecol. Evol., **6**, 32 (1991)

Arditi, R., Ginzburg, L.R.: Coupling in predator–prey dynamics: ratio-dependence. J. Theor. Biol., **139**, 311–326 (1989)

Arditi, R., Ginzburg, L.R., Akçakaya, H.R.: Variation in plankton densities among lakes: a case for ratio-dependent predation models. Am. Nat., **138**, 1287–1296 (1991)

Arditi, R., Ginzburg, L.R., Perrin, N.: Scale invariance is a reasonable approximation in predation models – reply to Ruxton and Gurney. Oikos, **65**, 336–337 (1992)

Arditi, R., Michalski, J.: Nonlinear food web models and their responses to increased basal productivity. In: Polis, G.A., Winemiller, K.O. (eds) Food Webs: Integration of Patterns and Dynamics. Chapman and Hall, New York, pp. 122–133 (1996)

Arnold, V.I.: Geometrical Methods of Ordinary Differential Equations. Springer-Verlag, New York (1983)

Bazykin, A.D.: (1998) Nonlinear Dynamics of Interacting Populations. Series on Nonlinear Science, Chua, L.O. (ed), Series A, vol. 11. World Scientific. [Original Russian version: Bazykin, A.D. Nauka, Moscow (1985)

Beddington, J.R.: Mutual interference between parasites or predators and its effect on searching efficiency. J. Anim. Ecol., **44**, 331–340 (1975)

Beretta, A., Kuang, Y.: Global analysis in some delayed ratio-dependent predator–prey systems. Nonlinear Analysis, Theory, Methods and Applications, **32**, 381–408 (1998)

Berezovskaya, F.S.: About asymptotics of trajectories of a system of two differential equations. Report deposited in the All-Union Information Center (USSR), No 3447-76, p 17, (1976) (in Russian)

Berezovskaya, F.S.: The main topological part of plane vector fields with fixed Newton diagram. In: Proceedings on Singularity Theory, Le, D.T., Saito, K., Teissier, B. (eds), Word Scientific, Singapore, New Jersey, London, Hong Kong. 55–73 (1995)

Berezovskaya, F.S., Medvedeva, N.B.: A complicated singular point of “center-focus” type and Newton diagram. Selecta Mathematica formerly Sovietica, vol. **13**(1), 1–15 (1994)
Cosner, C.: Variability, vagueness and comparison methods for ecological models. Bull. Math. Biol., **58**, 207–246 (1996)
Cosner, C., DeAngelis, D.L., Ault, J.S., Olson, D.B.: Effects of spatial grouping on the functional response of predators. Theor. Pop. Biol., **56**, 65–75 (1999)
DeAngelis, D.L., Goldstein, R.A., O’Neill, R.V.: A model for trophic interactions. Ecology, **56**, 881–892 (1975)
Diehl, S., Lundberg, P.A., Gardfjell, H., Oksanen, L., Persson, L.: *Daphnia*-phytoplankton interactions in lakes: Is there a need for pragmatic consumer-resource models? Am. Nat., **142**, 1052–1061 (1994)
Dulac, M.: Sur les cycles limites. Bull. Soc. Math. France. **51**, 45–188 (1923)
Freedman, H.I., Mathsen, R.M.: Persistence in predator–prey systems with ratio-dependent predator influence. Bull. Math. Biol., **55**, 817–827 (1993)
Hanski, I.: The functional response of predators: worries about scale. Trends Ecol. Evol., **6**, 141–142 (1991)
Hassell, M.P., Varley, C.C.: New inductive population model for insect parasites and its bearing on biological control. Nature, **223**, 1133–1137 (1969)
Hsu, S.-B., Hwang, T.-W., Kuang, Y.: Global analysis of the Michaelis-Menten type ratio-dependent predator–prey system. J. Math. Biol. in press (2001)
Huffaker, C.B.: Experimental studies on predation: dispersion factors and predator–prey oscillations. Hilgardia, **27**, 343–383 (1958)
Jost, C., Arino, O., Arditi, R.: About deterministic extinction in ratio-dependent predator–prey models. Bull. Math. Biol., **61**, 19–32 (1999)
Khibnik, A.I., Kuznetsov, Yu.A., Levitin, V.V., Nikolaev, E.V.: Continuation techniques and interactive software for bifurcation analysis of ODEs and iterated maps. Physica D, **62**, 360–371 (1993)
Kuang, Y.: Rich dynamics of Gause-type ratio-dependent predator–prey system. Fields Inst. Comm., **21**, 325–337 (1999)
Kuang, Y., Beretta, A.: Global qualitative analysis of a ratio-dependent predator–prey systems. J. Math. Biol., **35**, 389–406 (1998)
Kuznetsov, Yu.A.: Elements of Applied Bifurcation Theory. Applied. Math. Sci., vol. 112. Springer-Verlag, NY, Berlin, Heidelberg (1995)
Levitin, V.V.: TRAX: Simulation and analysis of dynamical systems. Exeter Software, Setauket, NY (1989)
Luck, R.F.: Trends. Ecol. Evol. **5**, 196–199 (1990)
Luckinbill, L.S.: Coexistence in laboratory populations of *Paramecium aurelia* and its predator *Didinium nasutum*. Ecology, **54**, 1320–1327 (1973)
Michalski, J., Arditi, R.: Food web structure at equilibrium and far from it: is it the same? Proc. R. Soc. Lond. B. **259**, 217–222 (1995)
Michalski, J., Poggiale, J.-C., Arditi, R., Auger, P.M.: Macroscopic dynamic effects of migration in patchy predator–prey systems. J. Theor. Biol., **185**, 459–474 (1997)
Poggiale, J.-C., Michalski, J., Arditi, R.: Emergence of donor control in patchy predator–prey systems. Bull. Math. Biol., **60**, 1149–1166 (1998)
Poletaev, I.A.: On mathematical models of elementary processes in biogeocoenosis. Problems of Cybernetics, No **16**, 171–190 (1966) (in Russian).
Rosenzweig, M.L.: Paradox of enrichment: destabilization of exploitation systems in ecological time. Science **171**, 385–387 (1971)
Ruxton, G.D., Gurney, W.S.C.: The interpretation of tests for ratio-dependence. Oikos, **65**, 334–335 (1992)
Sarnelle, O.: Inferring process from pattern: trophic-level abundances and imbedded interactions. Ecology, **75**, 1835–1841 (1994)